Reprocessing Effects on Polypropylene/Silica Nanocomposites

Andrea Dorigato,[1,2] Alessandro Pegoretti[1,2]

[1]Department of Industrial Engineering, University of Trento, Via Mesiano 77, 38123 Trento, Italy
[2]INSTM Research Unit, University of Trento, Via Mesiano 77, 38123 Trento, Italy
Correspondence to: A. Dorigato (E-mail: andrea.dorigato@ing.unitn.it)

ABSTRACT: A polypropylene matrix was melt compounded with a given amount (2 vol %) of both untreated (hydrophilic) and surface treated (hydrophobic) fumed silica nanoparticles with the aim to investigate the influence of the time under processing conditions on the microstructure and thermo-mechanical properties of the resulting materials. Chain scission reactions induced by thermal processing caused a remarkable decrease of the melt viscosity, as revealed by the melt flow index values of both neat matrix and nanocomposites, but the degradative effect was significantly hindered by the presence of silica nanoparticles. It was observed that the size of nanofiller aggregates noticeably decreased as the compounding time increased, especially when hydrophobic silica nanofiller was considered. While the melting temperature seemed to be unaffected by the processing time, a remarkable embrittlement of the samples was observed for prolonged compounding times. © 2013 Wiley Periodicals, Inc. J. Appl. Polym. Sci. **2014**, *131*, 40242.

INTRODUCTION

The addition of inorganic nanoparticles (such as silica, titania, carbon nanotubes, layered silicates etc.) at limited filler amounts (<5 wt %) has been proven to be extremely effective in increasing the physical properties of polymer matrices,[1] with noticeable beneficial effects in terms of dimensional stability,[2] moisture, and gas barrier properties,[3] enhanced mechanical resistance,[4–7] and flame retardancy.[8] Since, the first industrial application of polymer nanocomposites,[9] several efforts have been made to introduce novel nanocomposite systems through the combination of various polymeric matrices and nanofillers.[10]

Because of its high impact strength, elevated tensile strength, good chemical resistance, low density, and also rather low cost, polypropylene (PP) is one of the most widely used thermoplastics.[11] It is widely applied in the production of fibers, films for food packaging, bottles, and tubes. It has been demonstrated that the introduction of relatively small amounts of inorganic nanostructured materials in PP can effectively improve its chemical and mechanical stability.[12]

Quite surprisingly, less attention was devoted to PP-based nanocomposites filled with isodimensional nanofillers, such as fumed silica nanoparticles. From a morphological point of view, fumed silica nanoparticles are characterized by a wide range of specific surface area (from 50 to 400 $m^2 g^{-1}$) and by a variety of surface treatments from hydrophilic to hydrophobic. Because of its elevated specific surface area, fumed silica tends to self-aggregate

when dispersed in polymer matrices, forming an interconnected network of interacting particles.[13] In some articles, it has been demonstrated how fumed silica nanoparticles are very effective in increasing the fracture toughness and the tensile performance of PP.[14–16] In particular, it was found that the mechanical behavior PP/fumed silica nanocomposites is strongly affected by the filler content and by the presence of a surface functionalization.[17,18]

Very limited information is available on the effects of thermal reprocessing on the properties of nanofilled thermoplastics,[19–24] even if this aspect is surely important to establish the possibility to recycle thermoplastic nanocomposites. Chow et al.,[20] investigated the effect of a second extrusion on the mechanical behavior of poly(butylene-terephtalate) composites filled with an organomodified montmorillonite (MMT). It was reported that thermal reprocessing of nanocomposite samples did not substantially affect the original stiffness and the crystallization behavior of the material. Thompson and Yeung[19] performed a multiple-extrusion study on the recyclability of a layered silicate-thermoplastic olefin elastomer nanocomposite, observing that, despite the occurrence of degradation in the nanocomposite during recycling, both the rheological and the mechanical properties remained significantly higher than those of the neat matrix. Also Karahaliou and Tarantili[22] in a paper on the thermal reprocessing of acrilonitrile-butadiene-styrene/MMT nanocomposites showed how nanofiller introduction marginally influenced the rheological and the mechanical properties of reprocessed samples.

To the best of our knowledge, only Touati et al.[23] investigated the effects of reprocessing cycles on the structure and properties of PP based nanocomposites, reporting that the better dispersion of nanoclay in the nanocomposite induced by repeated extrusion cycles did not necessarily increase the thermal and the mechanical properties of the resulting material, because of the negative effect played by polymer degradation. In a preliminary work of our group, a linear low density polyethylene (LLDPE) matrix was melt compounded with both untreated (hydrophilic) and surface treated (hydrophobic) fumed silica nanoparticles, with the aim to investigate the influence of the thermal reprocessing on the microstructural and thermo-mechanical properties of the resulting materials.[25] It was demonstrated how crosslinking reactions induced by thermal processing determined a remarkable increase of the melt viscosity in all the tested samples, and the thermal oxidation of the matrix was slightly reduced upon silica introduction, especially for long compounding times. DSC tests evidenced how silica nanoparticles had a nucleating effect on the matrix, while both the melting temperature and the relative crystallinity were decreased by the compounding process. Also the tensile properties were positively affected by nanosilica addition.

Starting from these considerations, in the present work neat PP and nanocomposite samples filled with 2 vol % of both hydrophilic and hydrophobic fumed silica nanoparticles were prepared through a melt compounding process. The effect of the thermal reprocessing was modeled considering different compounding times, and the resulting materials were characterized by rheological tests, scanning electron microscopy, infrared spectroscopy, thermal and mechanical analyses.

EXPERIMENTAL

Materials

A PP Moplen® HP500H was kindly supplied by Basell Industries Italia Srl (Ferrara, Italy). This PP resin is characterized by a melt flow index (MFI) (at 230°C, 2.16 kg) equal to 1.8 g·(10 min)$^{-1}$ and a density of 0.90 g cm^{-3}. Two different kinds of Aerosil® fumed silica were provided by Degussa (Hanau, Germany). Aerosil® 200 (A200) is an hydrophilic fumed silica, having a density of 2.28 g cm^{-3} and a surface area of 200 m^2 g^{-1}. Aerosil® R974 (R974) silica nanoparticles are surface treated with dimethyldyclorosilane and has a density of 1.99 g cm^{-3} and a surface area of 170 m^2 g^{-1}. For both nanoparticles the SiO$_2$ content is higher than 99.8%. Both PP chips and fumed silica were utilized as received.

Preparation of the Samples

A melt compounding process followed by hot pressing was adopted for sample preparation. A Thermo Haake® internal mixer was used for compounding 2 vol % of both A200 and R974 silica nanoparticles in PP at 190°C and 60 rpm. Different compounding times, ranging from 5 to 60 min (virtually corresponding to 12 cycles of 5 min), were used to simulate thermal reprocessing operations. The resulting materials were then hot pressed in a Carver® press at 190°C for 10 min at a pressure of 0.2 kPa, to produce square sheets of 200 × 200 mm^2 about 0.8 mm thick. The choice of the filler amount was performed on the basis of the indications reported in our previous articles

on polyethylene/silica nanocomposites.[25–27] The samples were designated as PP followed by the silica type and the compounding time in minutes. For instance, PP-A200-5 denotes a nanocomposite sample filled with 2 vol % of Aerosil® 200 fumed silica and processed for a time of 5 min.

Measurements

MFI measurements were performed by a Dynisco 4003DE melt indexer, according to ASTM D1238 standard. Compounded materials were then pelletized and heated at 230°C, and MFI was measured under an applied weight of 2.16 kg. At least 10 measurements were made for each sample.

Field emission scanning electron microscope (FESEM) observations were performed through a Zeiss Supra 40 microscope, operating at an acceleration voltage of 10 kV. Samples were cryofractured in liquid nitrogen and observed at different magnifications after metallization. Fourier transform infrared spectroscopy (FTIR) tests were carried out by using a Perkin Elmer Spectrum One FTIR-ATR analyzer in a scanning interval between 650 and 4000 cm^{-1}. Differential scanning calorimetry (DSC) tests were performed through a Mettler® DSC30 apparatus on specimens having a mass of about 30 mg. A first heating scan from −40 to 240°C was followed by a cooling scan from 240 to −40°C and a second heating scan from −40 to 240°C. All scansions were performed at a rate of 10°C min^{-1} under a nitrogen flow of 100 ml min^{-1}. The relative crystallinity degree was determined normalizing the melting enthalpy over the standard enthalpy of a fully crystalline PP, taken as 207 J g^{-1}.[28]

Quasi-static tensile tests were performed by using an Instron® 4502 tensile testing machine, equipped with a load cell of 1 kN, on ISO 527 1BA dog bone specimens 5 mm wide and 0.8 mm thick. Elastic modulus was evaluated at a crosshead speed of 0.25 mm min^{-1}, and the strain was recorded by an Instron 2620–601 extensometer with a gage length of 12.5 mm. According to ISO 527 standard, the elastic modulus (E) was computed as a secant value between deformation levels of 0.05% and 0.25%. Tensile stress at yield (σ_y) and strain at break (ε_b) were determined at a crosshead speed of 50 mm min^{-1}, without using the extensometer, and the deformation was computed by normalizing the crosshead displacement over the gage length of the samples. At least five specimens were tested for each composition.

RESULTS AND DISCUSSION

Melt Flow Index

It is known that melt rheology of thermoplastic materials is strongly influenced by the molecular weight and/or by the polydispersity degree and that prolonged thermal treatments could strongly affect the molecular architecture.[29] The evaluation of the MFI can be very useful in order to obtain information on the effects of the thermo-mechanical degradative action promoted by melt compounding and the molecular weight distribution of the prepared samples. The trends of the MFI values of the neat matrix and of the relative nanocomposites with the processing time are reported in Figure 1. It can be observed that MFI values of neat PP strongly increase with the compounding time, with values of 1.75 g min^{-1} after a
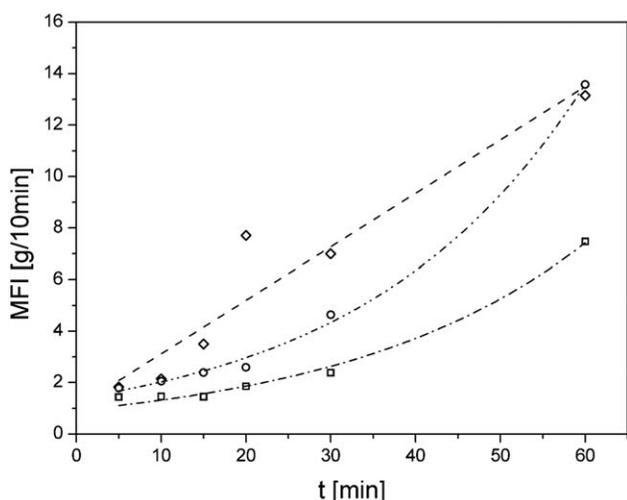
Figure 1. Melt flow index (MFI) values as a function of the processing time for neat PP-t ($\diamond$), PP-A200-t ($\square$), and PP-R974-t ($\bigcirc$) samples ($t = 5$–60 min).

compounding interval of 5 min up to 13 g min^{-1} after a processing duration of 60 min. According to the literature indications, the observed increase of the MFI can be related to the molecular weight decrease induced by chain scission reaction. In fact, the degradative action of a thermal treatment in polyolefins promotes the formation of alchilic radicals (R^{*}) through the rupture of covalent bonds, followed by the reaction with oxygen to form hydroperoxides (ROOH) through a chain reaction.[25] The oxygenated groups can be alcohols, aldehydes, ketones, acids, and esters. The addition of both kinds of fumed silica nanoparticles determines a noticeable decrease of the MFI values with respect to the unfilled matrix, especially at elevated compounding times. The increase of the melt viscosity due to nanoparticles introduction is a well known phenomenon,[13,30] and it is generally related to the formation of a percolative network between silica aggregates. It is interesting to note that MFI values of nanofilled samples are systematically lower than that of the neat PP over the whole range of the investigated compounding times. It could be therefore hypothesized that chain scission reactions due to thermal degradation are partially hindered by the presence of silica nanoparticles. It is interesting to observe that hydrophilic fumed silica nanoparticles are more effective than the hydrophobic ones in stabilizing the MFI values at prolonged processing times. According to some Refs. 31,32, this difference could be attributed to the relatively high amount of thermally less stable organic species introduced through surface treated silica, leading to the formation of low viscosity oligomers within the PP matrix.

Microstructure

In Figure 2(a–f) FESEM images of the fracture surfaces of neat PP and of the nanofilled samples with a compounding time of 5 and 60 min are reported. The surface corrugation of fracture surfaces is due to the relatively high ductility of PP, and the consequent difficulty to obtain a brittle fracture profile even under cryogenic conditions. The micrographs of PP-A200-5 nanocomposites [Figure 2(c)] evidenced how fumed silica
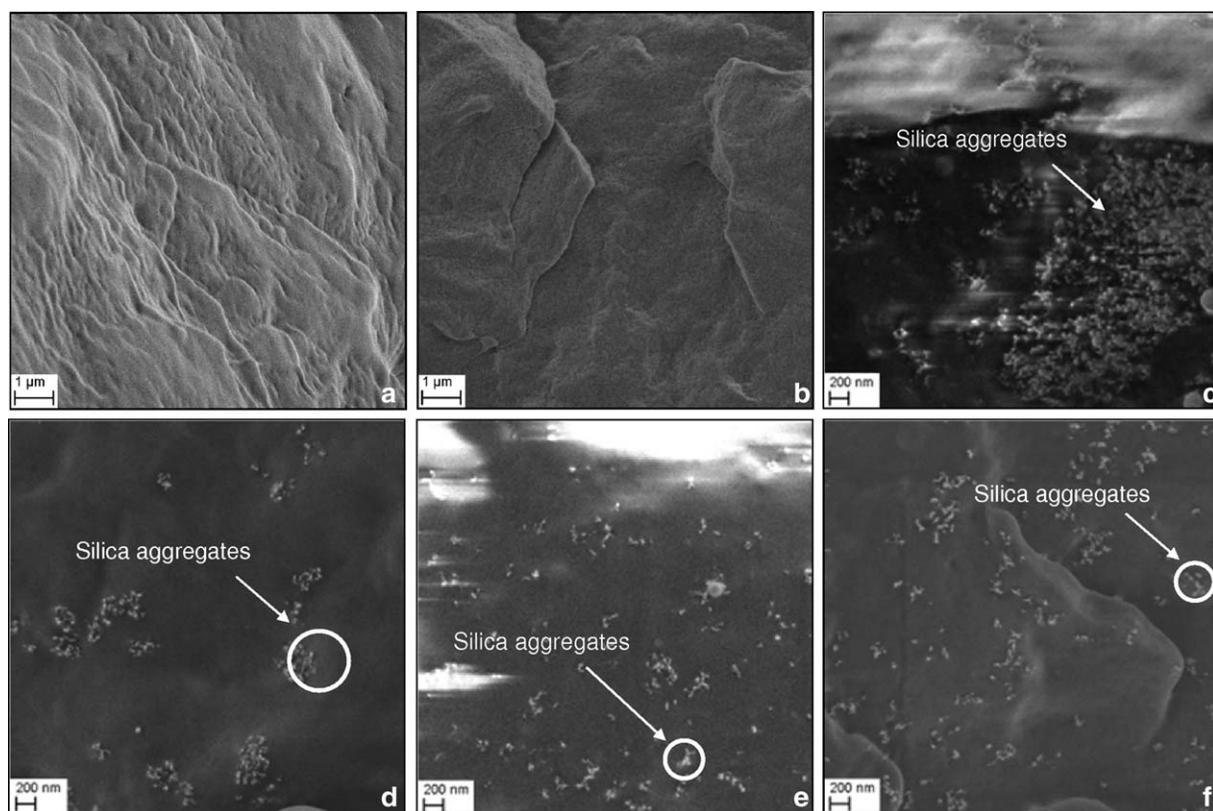

Figure 2. FESEM images of the fracture surfaces of (a) PP-5, (b) PP-60, (c) PP-A200-5, (d) PP-A200-60, (e) PP-R974-5, and (f) PP-R974-60 samples.
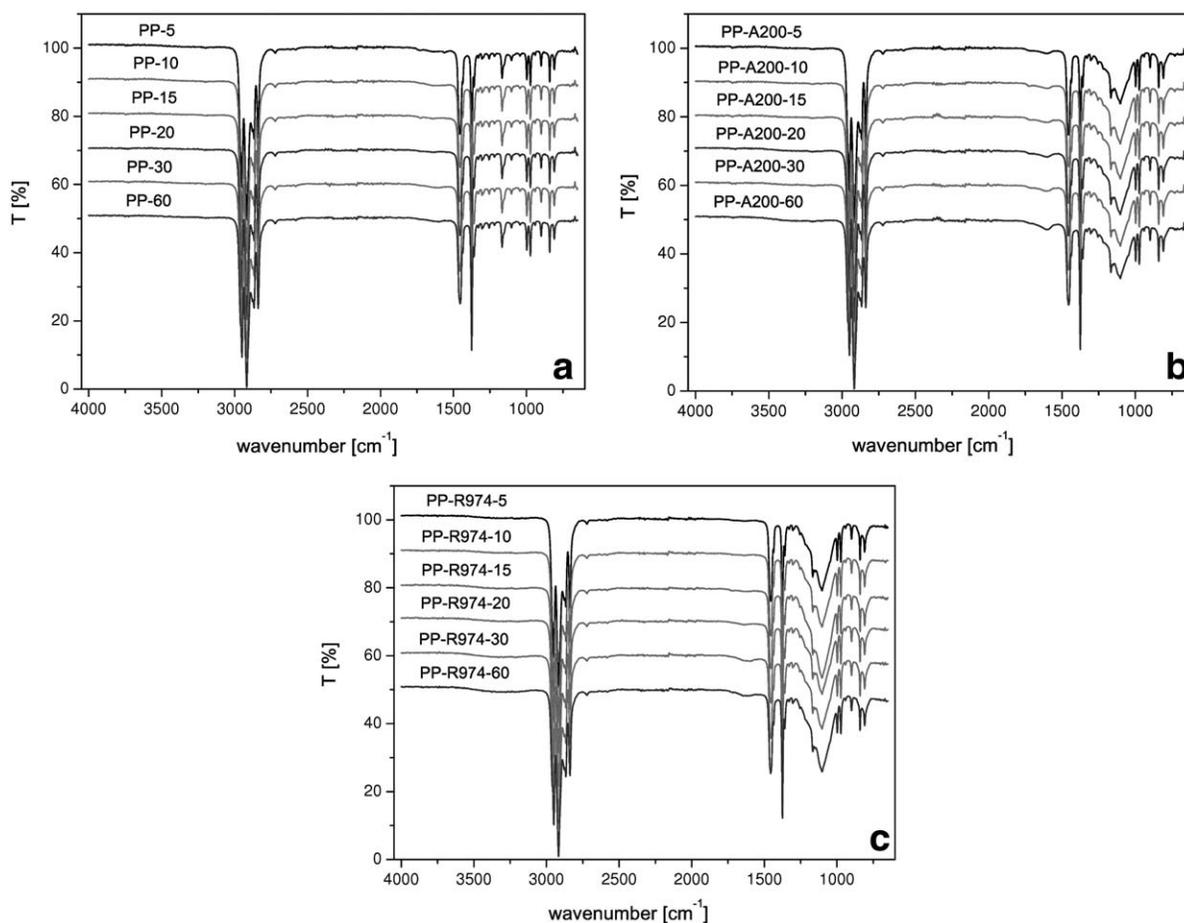
Figure 3. FTIR spectra of (a) PP-t, (b) PP-A200-t, and (c) PP-R974-t samples ($t = 5$–60 min).

nanoparticles are uniformly dispersed within the matrix, forming isodimensional aggregates of primary nanoparticles with a mean diameter of about 400 nm. As reported in our previous work on LLDPE nanocomposites,[13,30,33] this aggregated morphology is characteristic of fumed silica, and can be related to the strong interaction between the surface hydroxyl groups of the nanoparticles. The presence of an agglomerated morphology in these samples could be probably ascribed to the difficulties in nanofiller dispersion due to the relatively high viscosity of the polymer matrix. When a compounding time of 60 min is considered, a certain disgregation of the silica aggregates can be observed [Figure 2(d)]. For these samples, the mean dimension of silica aggregates is reduced down to about 300 nm. Therefore, a prolonged compounding time leads to a better nanosilica dispersion within the matrix, probably because of the decrease of the matrix viscosity induced by thermal degradation. As expected, a better dispersion with a reduction of the aggregates average dimension can be observed when surface functionalized nanoparticles are considered. In fact, from Figure 2(e,f) it can be observed that the mean size of the aggregates is reduced down to 150 nm, regardless to the compounding duration. Even in this case, a slight reduction of the silica aggregates can be obtained at elevated processing times. In the open scientific literature it is often reported that the surface treatment of

inorganic fillers with organic surfactants or coupling agents could lead to a decrease of their surface free energy and thus of their wettability.[34] In these conditions, interparticle interactions are reduced and the nanofiller dispersion within the matrix improved.

FTIR Analysis

As explained before, the presence of oxygenated functionalities in the material could be an indication of the thermal oxidation reaction induced by a prolonged thermal processing. FTIR spectroscopy could be therefore a very sensitive technique to investigate the evolution of the thermo-oxidative degradation process. Figure 3 reports FTIR spectra of neat matrix [Figure 3(a)] and of the nanofilled samples [Figures 3(b,c)] at different compounding times. IR spectra of neat PP samples are characterized by the presence of two characteristic absorbance peaks at about 2900 and 1455 cm^{-1}, respectively associated to the stretching of the C—H bonds and to the bending of CH$_2$ groups. Moreover, an absorbance signal at 1376 cm^{-1}, related to the symmetric bending of CH$_3$ group, can be detected in all the samples.[35] On FTIR spectra of the nanocomposites [Figures 3(b,c)] the presence of two peaks at 1105 and 802 cm^{-1}, respectively attributable to the asymmetric and symmetric stretching of Si—O—Si groups, can be noticed. Interestingly, an increase of the
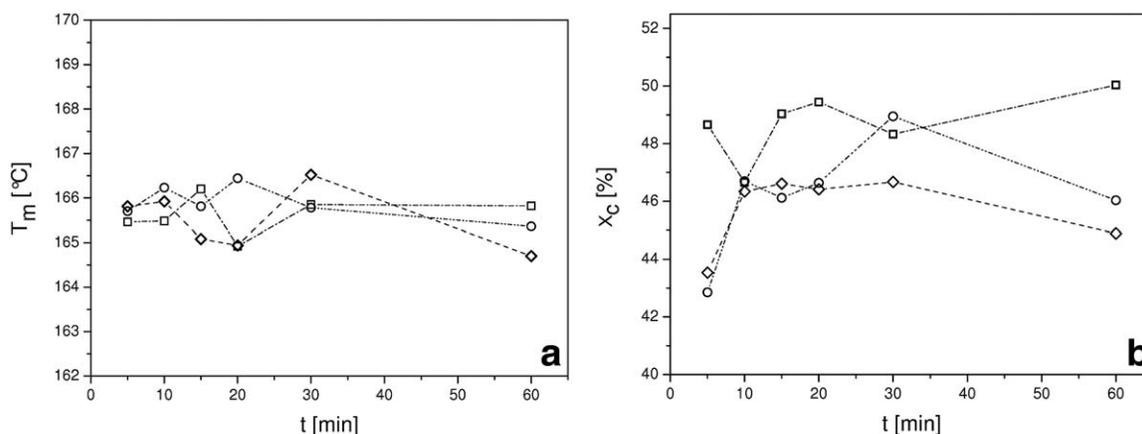
Figure 4. Results of DSC first heating scan on (◇) PP-t, (□) PP-A200-t, and (○) PP-R974-t samples ($t = 5$–60 min). (a) Melting temperature and (b) Crystallinity degree.

compounding time does not determine any substantial variation in the FTIR spectra of the tested materials. This probably means that thermal degradation of the polymer matrix leads to a decrease of the molecular weight, but does not introduce oxygenated functionalities in the main backbone of PP, as often reported for polyolefins.[36,37] The same conclusion can be drawn also for nanofilled samples, regardless the presence of a surface compatibilizer. Different results were found in our previous article on the thermal reprocessing of LLDPE based nanocomposites. In that case, an absorbance peak located at 1720 cm^{-1}, attributed to the stretching of carbonyl groups (C=O), could be detected at elevated compounding time, and the introduction of silica nanoparticles noticeably limited LLDPE oxidation.

Differential Scanning Calorimetry

It is well known that thermal degradation could significantly affect thermal properties of polyolefins, and the introduction of inorganic nanofillers can affect both the melting and the crystallization behavior of the PP matrix. The dependency of the melting temperature (T_m) of neat PP and of the relative nanocomposites from the compounding time was evaluated through DSC tests. The results obtained from the first heating scan are reported in Figure 4(a), while in Figure 4(b) the crystallinity content (χ_C) is reported. While the melting temperature seems to be unaffected both by the compounding time and by fumed silica introduction, nanofiller addition determines a slight increase of the crystallinity degree, especially in the case of untreated nanoparticles. This probably means that, despite their amorphous nature, fumed silica nanoparticles can probably promote a nucleating effect on the PP matrix. The role played by inorganic nanoparticles on the crystallization properties of polyolefins is still debated in the scientific literature,[38–40] and some controversial results were reported in our previous works on polyethylene based nanocomposites.[12,13] According to the mechanism proposed by Ebengou,[41] it can be hypothesized that in nanofilled samples PP chains are preferentially adsorbed on the silica surface, because of the decrease of their configuration entropy. In these conditions, the formation of the critical volume required for polymer crystallization is promoted. However, a deeper investigation about the effect of particle type and

processing time on the crystallization behavior of the prepared samples should require other experimental techniques, such as XRD analysis. On the other hand, a detailed description of the crystalline behavior of these nanocomposites is out from the main scope of the present work.

Mechanical Properties

Representative stress–strain curves of neat PP at different processing times, derived from quasi-static tensile tests, are represented in Figure 5. It is clear that as the processing time increases a considerable modification of the mechanical response occurs, especially if the ultimate properties are considered. The values of the most important tensile properties are plotted in Figure 6(a–c) at various compounding times for both neat PP and nanocomposites. As for as the elastic modulus is concerned, it can be concluded that the stiffness of the tested samples is practically unaffected by the compounding time. It could be interesting to note that the introduction of untreated nanoparticles leads to a slight decrease of the material stiffness, while the addition of hydrophobic silicas determines a systematic increment of the elastic modulus with respect to the neat PP. Even if a more detailed analysis should be performed in order to have a complete explanation of this result, the observed
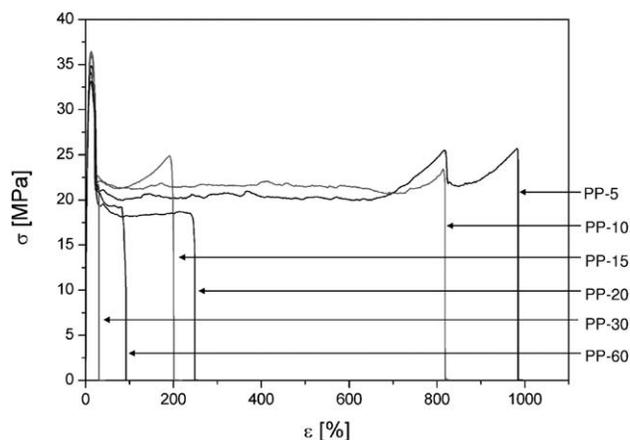

Figure 5. Representative stress–stain curves on PP-t samples ($t = 5$–60 min).
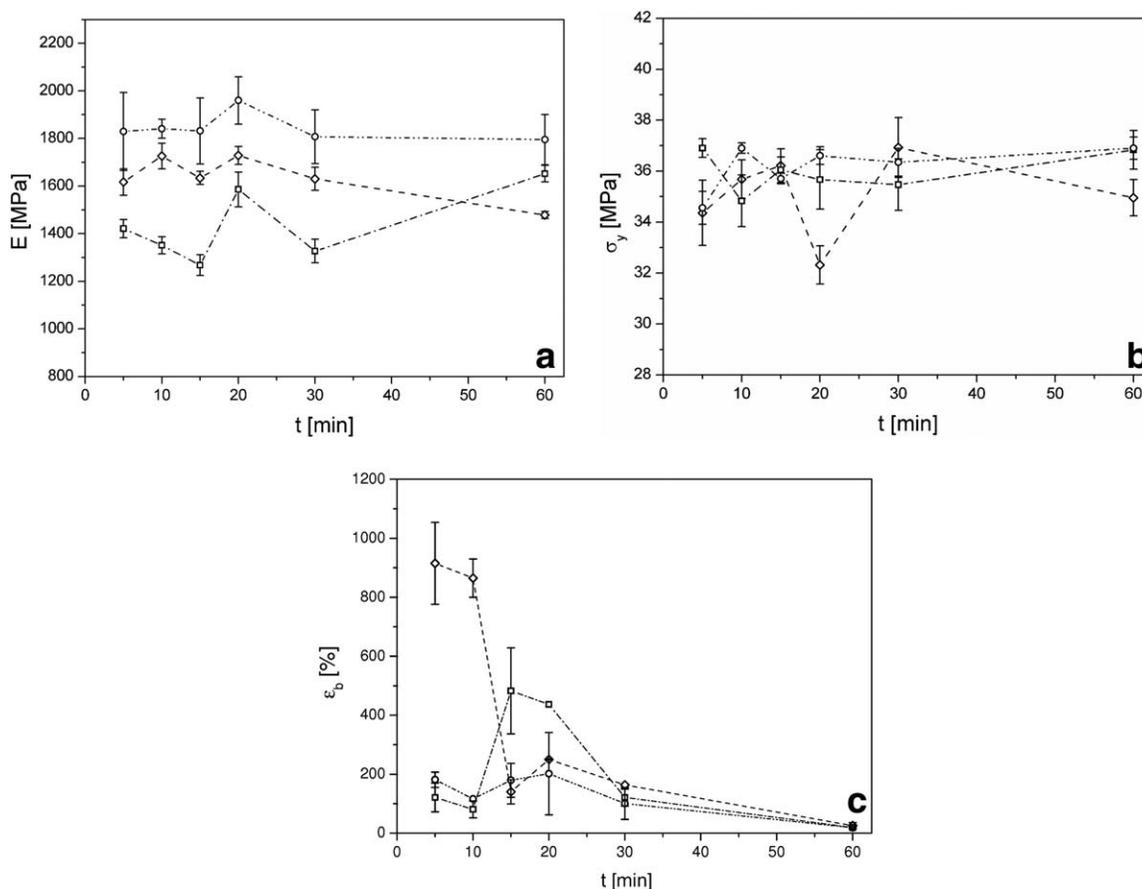
Figure 6. (a) Elastic modulus, (b) stress at yield, and (c) strain at break of ($\diamond$) PP-t, ($\square$) PP-A200-t, and ($\bigcirc$) PP-R974-t samples ($t = 5$–60 min).

difference could be ascribed to the peculiar morphological features of the tested samples. FESEM images reported in Figures 2(a–f) demonstrated how the presence of the surface functionalization leads to an important reduction of the silica aggregates, regardless the compounding time. The higher stiffness observed in nanocomposites filled with R974 nanoparticles can be therefore attributed to a better dispersion of the nanofiller aggregates within the matrix. The strong dependency of the material stiffness of polymer nanocomposites from the filler aggregation was highlighted in a recent article of our group, in which a new theoretical model was proposed to model the elastic properties of particulate nanocomposites.[42,43] In that work, it was evidenced how nanofiller aggregation may constrain a portion of matrix, thus limiting the mobility of macromolecules and providing a stiffening effect. A modification of the aggregative state of the nanoparticles could be therefore responsible of the variations of the elastic modulus observed for the tested materials. It is also worthwhile to analyze the trends of the ultimate properties with the processing time. While from Figure 6(b) it can be observed how the stress at yield is practically unaffected by the compounding time and by the presence of the nanofiller, more interesting information can be obtained from Figure 6(c), in which strain at break data are collected. An increase of the processing time in PP leads to a dramatic reduction of the deformation at break, probably because of the

molecular weight decrease induced by thermal degradation. Even the introduction of silica nanoparticles leads to a strong embrittlement of the samples due to the immobilizing effects on the macromolecular chains. Therefore, an increase of the processing time in nanocomposite samples does not produce a further decrease of material ductility as experienced for neat PP. In fact, after a compounding time of 360 min ε_b values of nanofilled samples are practically equal to that of the neat matrix.

CONCLUSIONS

Both hydrophilic and surface treated fumed silica nanoparticles were melt compounded in a PP matrix, in order to investigate the influence of the processing duration on the thermomechanical behavior of the resulting materials. MFI measurements evidenced how the viscosity of both neat PP and the nanofilled samples progressively decreased with the processing time, due to chain scission reactions induced by thermal reprocessing, but the degradation rate was noticeably reduced upon hydrophilic silica introduction. The nanofiller dispersion within the matrix was noticeably improved for long compounding times, especially when hydrophobic fumed silica nanoparticles were considered.

FTIR analysis evidenced how the thermal degradation of the polymer matrix was not associated to a significant introduction

of oxygenated functionalities in the main backbone of PP. DSC tests showed how nanosilica addition determined a slight increase of the crystallinity degree, especially in the case of untreated nanoparticles, while the melting temperature was practically unaffected both by the compounding time and by nanofiller introduction.

Quasi-static tensile tests highlighted how the stiffness of the tested samples was practically unaffected by the compounding time, while hydrophobic nanosilica introduction lead to a slight decrease of the material stiffness with respect to the neat PP. An increase of the processing time promoted a dramatic reduction of the deformation at break, probably because of the molecular weight decrease induced by thermal degradation, and also the introduction of silica nanoparticles lead to a strong embrittlement of the samples, due to the immobilizing effects on the macromolecular chains.

ACKNOWLEDGMENTS

REFERENCES

1. Bondioli, F.; Dorigato, A.; Fabbri, P.; Messori, M.; Pegoretti, A. *Polym. Eng. Sci.*, 48, 448 **2008**.

2. Bondioli, F.; Dorigato, A.; Fabbri, P.; Messori, M.; Pegoretti, A. *J. Appl. Polym. Sci. 112*, 1045, **2009**.

3. Kim, J. K.; Hu, C.; Woo, R. S. C.; Sham, M. L. *Compos. Sci. Technol. 65*, 805, **2005**.

4. Kontou, E.; Niaounakis, M. *Polymer 47*, 1267, **2006**.

5. Pegoretti, A.; Dorigato, A.; Penati, A. *Exp. Polym. Lett. 1*, 123, **2007**.

6. Pegoretti, A.; Dorigato, A.; Penati, A. *Eur. Polym. J. 44*, 1662, **2008**.

7. Dimitry, O. I. H.; Abdeen, Z. I.; Ismail, E. A.; Saad, A. L. G. *J. Polym. Res. 17*, 801, **2010**.

8. Zhang, J.; Jiang, D. D.; Wilkie, C. A. *Polym. Degrad. Stab. 91*, 358, **2005**.

9. Kojima, Y.; Usuki, A.; Kawasumi, M.; Kojima, Y.; Fukushima, Y.; Okada, A. *J. Mater. Res. 8*, 1185, **1993**.

10. Supova, M.; Martynkova, G. S.; Barabaszova, K. *Sci. Adv. Mater. 3*, 1, **2011**.

11. Phuong, N. T.; Gilbert, V.; Chuong, B. *J. Reinforc. Plast. Compos. 27*, 1983, **2008**.

12. Dorigato, A.; Pegoretti, A.; Kolarik, J. *Polym. Compos. 31*, 1947, **2010**.

13. Dorigato, A.; Pegoretti, A.; Penati, A. *Exp. Polym. Lett. 4*, 115, **2010**.

14. Wu, C. L.; Zhang, M. Q.; Rong, M. Z.; Friedrich, K. *Compos. Sci. Technol. 62*, 1327, **2002**.

15. Wu, C. L.; Zhang, M. Q.; Rong, M. Z.; Friedrich, K. *Compos. Sci. Technol. 65*, 635, **2005**.

16. Rong, M. Z.; Zhang, M. Q.; Pan, S. L.; Lehmann, B.; Friedrich, K. *Polym. Int. 53*, 176, **2004**.

17. Bikiaris, D. N.; Papageorgiou, G. Z.; Pavlidou, E.; Vouroutzis, N.; Palatzoglou, P.; Karayannidis, G. P. *J. Appl. Polym. Sci. 100*, 2684, **2006**.

18. Vladimirov, V.; Betchev, C.; Vassiliou, A.; Papageorgiou, G.; Bikiaris, D. *Compos. Sci. Technol. 66*, 2935, **2006**.

19. Thompson, M. R.; Yeung, K. K. *Polym. Degrad. Stab. 91*, 2396, **2006**.

20. Chow, W. S. *J. Appl. Polym. Sci. 110*, 1642, **2008**.

21. Goitisolo, I.; Equiazabal, J. I.; Nazabal, J. *Polym. Degrad. Stab. 93*, 1747, **2008**.

22. Karahaliou, E. K.; Tarantili, P. A. *J Appl Polym Sci 113*, 2271, **2009**.

23. Touati, N.; Kaci, M.; Bruzaud, S.; Grohens, Y. *Polym. Degrad. Stab. 96*, 1064, **2011**.

24. Kaci, M.; Remili, C.; Benhamida, A.; Bruzaud, S.; Grohens, Y. *Mol. Cryst. Liq. Cryst. 556*, 94, **2012**.

25. Dorigato, A.; Pegoretti, A. *J. Polym. Res. 20*, 92, **2013**.

26. Dorigato, A.; D'Amato, M.; Pegoretti, A. *J. Polym. Res. 19*, 9889, **2012**.

27. Dorigato, A.; Pegoretti, A. *Eng. Fract. Mech. 79*, 213, **2012**.

28. Mark, H. F. Encyclopedia of Polymer Science and Technology, 3rd edn.; Wiley: New York, **2004**.

29. Gupta, R. K. Polymer and Composite Rheology; Dekker: New York, **2000**.

30. Ajayan, P. M.; Schadler, L. S., Nanocomposite Science and Technology; Wiley-VCH: Weinheim, Germany, **2003**.

31. Leszczynska, A.; Njuguma, J.; Pielichowski, K.; Banerjee, J. R. *Thermochim. Acta 453*, 75, **2007**.

32. Garcia, N.; Hoyos, M.; Guzman, J.; Tiemblo, P. *Polym. Degrad. Stab. 94*, 39, **2009**.

33. Dorigato, A.; Pegoretti, A.; Frache, A. *J. Therm. Anal. Calorim. 109*, 863, **2012**.

34. Naveau, E.; Dominkovics, Z.; Detrembleur, C.; Jerome, C.; Harim, J.; Renner, K.; Alexandre, M.; Pukanszky, B. *Eur. Polym. J. 47*, 5, **2011**.

35. Silverstein, R. M.; Bussler, G. C.; Morril, T. C. Spectroscopic Identification of of Organic Compounds; Wiley: New York, **1981**.

36. Holmstrom, A.; Sorvik, E. *J. Appl. Polym. Sci. 18*, 3153, **1974**.

37. Holmstrom, A.; Sorvik, E. M. *J. Polym. Sci. Part A: Polym. Chem. 16*, 2555, **1978**.

38. La Mantia, F. P.; Dintcheva, N. T.; Scaffaro, R.; Marino, R. *Macromol. Mater. Eng. 293*, 83, **2008**.

39. Ruan, S.; Gao, P.; Yu, T. X. *Polymer 47*, 1604, **2006**.

40. Zhang, Y.; Yu, J.; Zhou, C.; Chen, L.; Hu, Z. *Polym. Compos. 31*, 684, **2010**.

41. Ebengou, R. H. *J. Polym. Sci. Part B: Polym. Phys. 35*, 1333, **1997**.

42. Dorigato, A.; Dzenis, Y.; Pegoretti, A. *Procedia Eng. 10*, 894, **2011**.

43. Dorigato, A.; Pegoretti, A.; Dzenis, Y. *Mech. Mater. 61*, 79, **2013**.